11th Canadian Masonry Symposium, Toronto, Ontario, May 31- June 3, 2009

UPGRADING THE SEISMIC PERFORMANCE OF REINFORCED MASONRY COLUMNS USING CFRP WRAPS

Nima Farnia[1] and Khaled Galal[2]

[1] Ph.D. Candidate, Dept. of Building, Civil & Environmental Engineering, Concordia University, Montréal, Québec, H3G 1M8, Canada, nima.farnia@gmail.com

[2] Associate Professor, Dept. of Building, Civil & Environmental Engineering, Concordia University, Montréal, Québec, H3G 1M8 Canada, galal@bcee.concordia.ca

ABSTRACT

Compared to reinforced concrete, relatively few experimental studies have been conducted to document the behaviour of masonry columns under combined axial load and flexure. Furthermore, by introducing new techniques such as using carbon fibre-reinforced polymers (CFRP) wraps, it is possible to enhance the behaviour of reinforced masonry columns considerably. Therefore, this paper focuses on improving the seismic performance of reinforced masonry columns using CFRP wraps. In current experimental study, three 1.4m reinforced masonry columns were constructed and tested when subjected to constant axial force and cyclic lateral excitations. The columns have a cross-section of 390mmx390mm and were constructed using bull-nosed concrete units. The first column, which had no CFRP wraps, was used as a control specimen while second and third columns were wrapped with 2 and 4 layers of CFRP sheets respectively. The columns were subjected to a constant axial force of 200 kN. From the tests, it was observed that CFRP wraps improves confinement of masonry column, which leads to more ductile behaviour and improvement in lateral load capacity.

KEYWORDS: reinforced masonry columns, CFRP wraps, seismic, and ductile behaviour.

INTRODUCTION

Many devastating and deadly earthquakes continuously occur around the world. In major earthquake events, losses are considerable due to buildings collapse and, consequently, human casualties. Lessons from these destructive earthquakes are continuously adding to our knowledge, and especially for masonry structures, there are many existing structures deficient to resist (or have a satisfactory performance) in future medium to high ground motions. Majority of these buildings have common deficiencies such as poor proportioning of members causing strong beam and weak columns, soft stories, or, non-ductile performance due to occurrence of short column mechanism.

For reinforced masonry columns and piers that are part of the moment resisting system, recent research showed that the confinement in such members especially near the potential plastic hinging regions is not enough [1]. Since demolishing and reconstructing such deficient elements is not an option, retrofitting them to meet appropriate seismic ductility demands is an engineering must.

For retrofitting and upgrading purposes, fibre-reinforced polymer (FRP) composite materials have become popular material in strengthening reinforced concrete elements in recent years. It offers attractive characteristics such as high strength and high stiffness–to-weight ratio, as well as light weight for ease of application with minimal interruption to occupants [2–4].

Most research efforts in retrofitting deficient masonry structural elements using FRP were directed to masonry walls and less work has been conducted in the past on retrofitting reinforced masonry columns. On the other hand, there has been significant effort in evaluating the performance of FRP-rehabilitated plain and reinforced concrete (RC) columns (e.g. [5–11]). In General, previous research showed that wrapping non-ductile RC columns with carbon FRP (CFRP) sheets is an effective form of increasing the column's ductile and, hence, seismic performance [10, 12]. In order to increase confinement, FRP wraps are laid perpendicular to the column axis. However, the wrap is not activated until the concrete is dilating substantially as it is failing [11]. Early research work on FRP-strengthening of RC columns concluded that FRP wrapping is more efficient in circular columns compared to rectangular ones due to stress concentration at the columns' edges. Chamfering round corners for concrete columns have been recommended to avoid such problem [15], where for masonry; bull-nosed units can be used for the corners of the columns [13]. It is observed in previous researches [11] that in wrapped masonry columns under only axial load, failure appeared to be initiated by complete crushing of the mortar joints, causing wrinkles in the wrap, followed by explosive disruption of the CFRP wrap. The material first rips vertically, then very rapidly circumferentially at failure of masonry columns.

In this experimental program, wrapped column were tested when subjected to constant axial load and increasing lateral excitations. It is noteworthy to say that, up to authors' knowledge, literature survey did not reveal similar experimental program on the behaviour of masonry columns under combined axial and lateral loads.

EXPERIMENTAL PROGRAM

In this research, the tests were carried out in two phases: a) the auxiliary tests that are meant to provide the mechanical characteristics of the constituent materials and the masonry assemblage, and b) Three 390x390x1400mm reinforced masonry columns were constructed and tested when subjected to constant axial force and cyclic lateral excitations. All the auxiliary specimens (masonry prisms) and columns were constructed by domestic professional masons representing the current method of practice in Québec.

Material properties of concrete masonry blocks, mortar, grout, compressive and tensile strength of masonry assemblage, and CFRP sheets are summarized in Tables 1(a) to 1(c). The steel rebars used as vertical reinforcement in the columns have the yield strength of 400 MPa. Stirrups of 4.65mm with a yield strength of 360 MPa where used as shear reinforcement. The masonry unit that is used in this study is hollow concrete block with two bull-nose corners with nominal dimensions of 390mmx190mmx190mm. The average tested compressive strength of the unit is 24 MPa and the average net-to-gross area ratio is 0.7. Type S mortar that is a mix of 0.5 volumetric unit Portland cement, one unit masonry cement, 2.9 units sand, and 0.7 unit water was chosen after several trial mixtures to be conforming with the requirements stated in ASTM C270-02 [16] and CSA A179-04 [17].

The grout used in the program, categorized as "coarse grout" in accordance with CSA A179-04 and ASTM C476-02 [18], was mixture of one volumetric unit Portland cement, 2.8 units fine aggregate (sand), two units coarse aggregates with the maximum size of 7mm (1/4″), and 0.9 unit of water.

Table 1(a): Compressive strength of constituent materials (MPa)

Bullnose masonry units	Type S mortar cubes	Coarse grout cylinders
15	20.7*	21.6*

* 28 days strength

Table 1(c): Properites of the Tyfo SCH-11UP wraps (as provided by the suplier, Fyfo Co. 2008)

Tensile strength (MPa)	Young's modulus (MPa)	Elongation at break (%)
903	86.9	1.05

Table 1(b): Mechanical properites of the masonry assemblage (MPa)

Compressive strength. Five-high prisms stacks (MPa)	11.5
Tensile strength .Seven-high prisms stacks (MPa)	1.29

Figure 1: Tests for obtaining compressive (left) and tensile (right) strength of masonry assemblage

In order to obtain compressive strength of masonry assemblage (f'_m) a series of five unreinforced grouted prisms were tested according ASTM C1314-02a [19] and as shown in Figure 1. It was decided to build five-block high and one-block wide prisms for a better representative of the real circumstances in the masonry columns.

For the purpose of estimating the tensile strength of the masonry assemblage, a series of five prisms were tested by third-point loading method according to ASTM E518-02 [20] guideline. As it is shown in Figure 1, Prisms with the height of seven blocks and width of one block were constructed in order to properly locate the two point loads and supports and also to provide sufficient span-to-depth ratio.

In the second phase of this experimental study, three 39x390x1400mm reinforced masonry columns were constructed on reinforced concrete footings which were fixed properly on strong floor to simulate fixed support condition. Each column was reinforced with four 15M vertical steel bars and 4.75mm steel stirrups on every row as shown in Figure 2. The first column was tested as control specimen without any CFRP wraps and second and third columns had one and two layers of full-height CFRP wraps, respectively. Table 2 shows the designation of the three tested columns. The tested columns were subjected to a constant axial force of 200kN ($\sigma = 0.11f'_m A_g$) and cyclic lateral excitations. Two cycles were applied at each displacement level. Figure 3 illustrates the loading history diagram of the second test for the column with 2 layers of CFRP wraps. Figure 4 shows a schematic of the test set-up and the location of potentiometers used for displacement measurement.

Table 2: Designation of specimens

Specimen	**Designation**
control specimen: **R**einforced **M**asonry **C**olumn	RMC-0
Reinforced **M**asonry **C**olumn with **1** layer of **C**FRP **W**raps	RMC-CW-1
Reinforced **M**asonry **C**olumn with **2** layers of **C**FRP **W**raps	RMC-CW-2

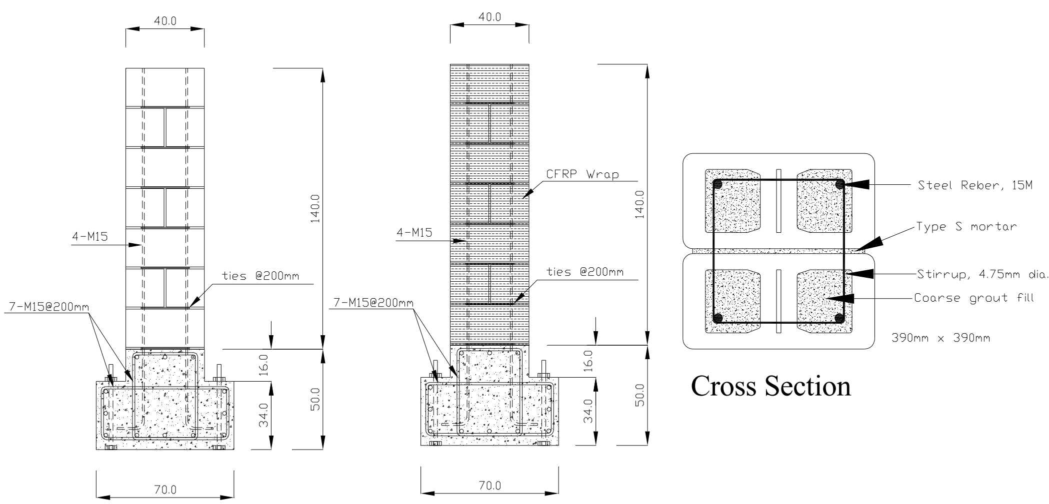

Specimen RMC-0 Specimens RMC-CW-2 & RMC-CW-1

Figure 2: Dimensions and details of reinforcement of the three tested columns

Instrumentation: The tested columns were instrumented to capture the displacement and strain measurements using a data acquisition system. Four strain gauges were installed on vertical rebars at the location of the base of each column. Two horizontal linear potentiometers were attached to each side of the column along the point of application of lateral load, and two horizontal potentiometers were attached to the column in order to measure the tip and mid height displacements. Three potentiometers were installed on the RC footing in order to ensure there has no rotation relative to the strong floor. Furthermore, three strain gauges were installed on bottom, middle, and top along the height of the column on the surface of CFRP wraps. Also, strain gauges were installed on bottom, middle, and top stirrups.

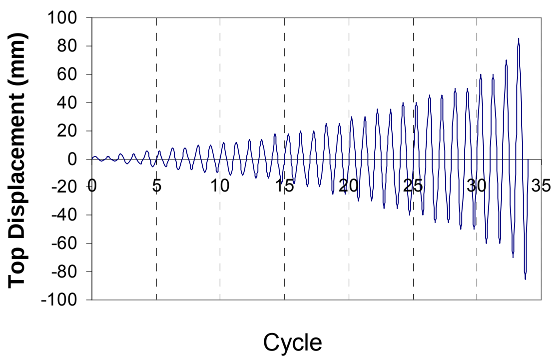

Figure 3: Displacement history

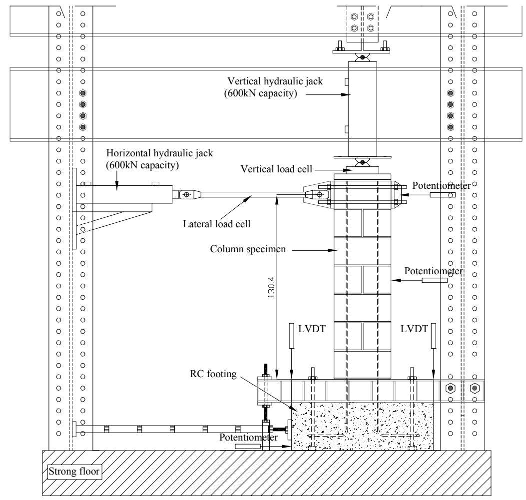

Figure 4: Test setup and instrumentation

TEST RESULTS

Analysis: Lateral force-deformation hysteretic relationship is a valuable indicative of the seismic performance of structural resistant elements. Due to the contribution of the horizontal component of the 200 kN vertical load to the lateral applied load (especially at high lateral displacements), the lateral load is calculated as:

$$F_{adj} = V + P.\frac{\Delta}{h_2} \tag{1}$$

where Δ is the lateral displacement of the tip of the column, and h_2 is the distance between two hinges on the top of the column. Note that since displacements are relatively small, contribution of vertical component of V was neglected in estimation of F_{adj} .

The test results are analyzed and plotted for each column in the following sections. The following figures were produced for each specimen:

1. Column pictures during the test and various drift levels. (see Figures 5, 7 and 9)
2. Adjusted lateral load versus drift ratio responses.(see Figures 6, 8 and 10)

Behaviour of column RMC-0: Prior to the application of lateral load, the control column was first loaded with a constant axial compressive force of 200 kN, corresponding to approximately 11% of the axial load capacity. Observations during testing showed that the first crack was formed at 0.7% drift level. The cracks were widened during the subsequent cycles at the same displacement. At 1.0% and 5% drift levels, new cracks appeared and continued to widen. The new diagonal cracks caused decrease in the load capacity. The maximum lateral load reached during the test was 62 kN at the 0.8% drift level (see Figure 6). Spalling of concrete blocks was observed at the base of the column at 4.0% drift level as it is shown in Figure 5. After completion of 2.0% drift level, column was only pushed until the end of the test at 5% drift level.

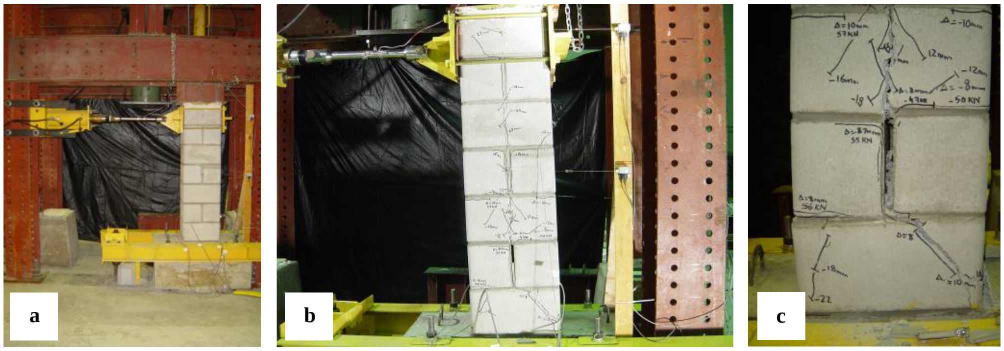

Figure 5: (a) Control specimen before test (b) Column at 2% drift level (c, d) Sample of cracks and spalling at column's base (e) Column at 5% drift level

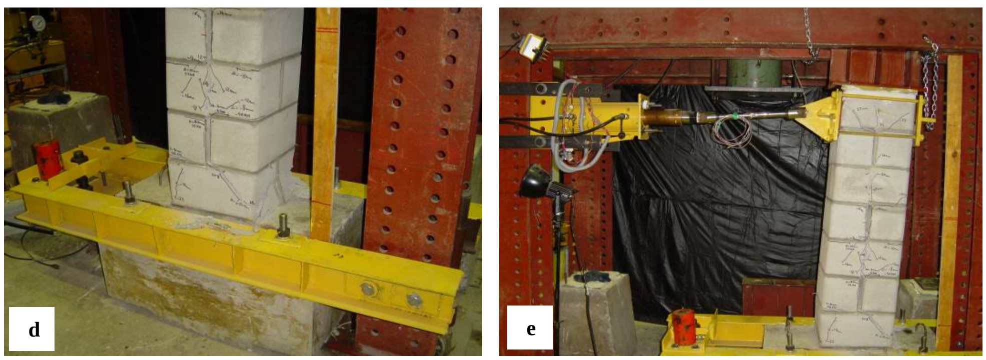

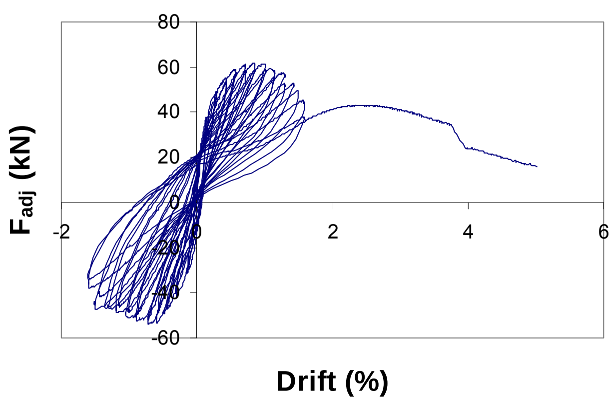

Figure 6: Lateral load versus drift

Behaviour of Column RMC-CW-1: In this test, due to the confinement provided by one layer of CFRP wraps it was not possible to monitor cracking or spalling of the original masonry column; however, in plastic hinge zone rupture of CFRP wrap and crushing of the blocks were observed at high level of lateral loads (Figure 7-c). Similar to two previous tests, axial load was kept on constant value of 200 kN. The lateral load did not increase after the drift level of 1.5% and reduced gradually after. The maximum lateral load reached during the test was 63 kN at the 1% drift level (see Figure 8). Test was stopped at 5% drift level, after observing that lateral load capacity has reduced to less than 80% of the maximum lateral load.

Figure 7: (a) Wrapped column before the test (b) Specimen at 5% drift level (c) Wrap rupture near the base

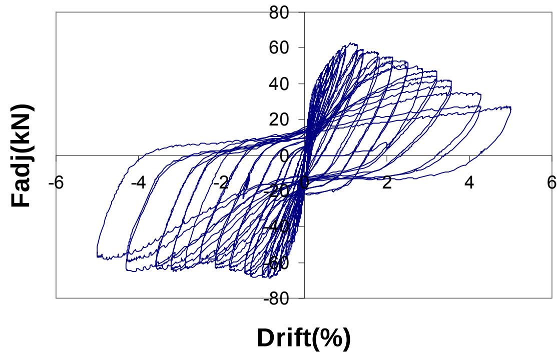

Figure 8: Lateral load versus drift (%)

Behaviour of Column RMC-CW-2: In last test, due to the confinement provided by 2 layers of CFRP wraps no cracking or spalling was observed on the surface of the column (Figure 9). After removing the CFRP sheets, it is observed that the cracks had been occurred at the intersection of the foundation and column. The load did not increase after the drift of 1% and reduced gradually after. Axial load was kept on 200 kN during the test. The maximum lateral load reached during the test was 76 kN at the 0.9% drift level (see Figure 10). Due to technical problems, it wasn't possible to continue the lateral drift beyond 6% drift, and up to this point no rupture or damage were occurred on CFRP wraps; however, local debonding of the wrap were observed. Note that after reaching to 5% drifts level, the specimen was only pushed up until the end of this test.

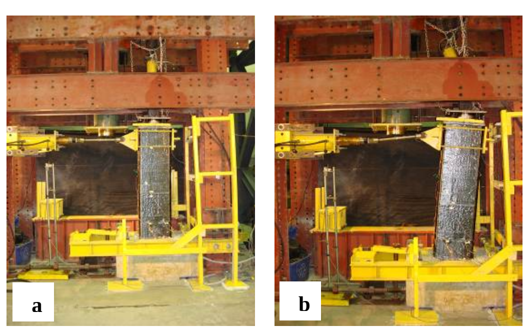

Figure 9: (a) Wrapped column before the test (b) Specimen at 6% drift level

Stiffness: Stiffness values were determined by dividing the maximum load reached within a cycle by the corresponding displacement in the positive or negative direction (see Figure 11). The stiffness of a cycle, K_{avg} is expressed by:

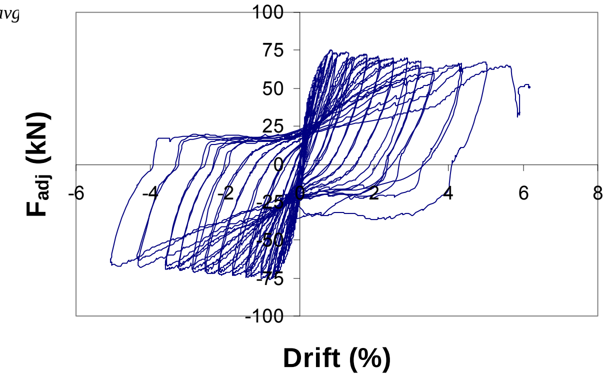

Figure 10: Lateral load versus drift

$$K_{avg} = \frac{K_{+} + K_{-}}{2} \tag{2}$$

where K_{+} and K_{-} are the stiffness values in positive and negative directions, respectively [21]. Stiffness degradation diagram for the three columns RMC-0, RMC-CW-1 and RMC-CW-2 are given in Figure 12. It was observed that retrofitted column (RMC-CW-2) exhibited higher stiffness values than non-retrofitted column (RMC-0) while stiffness degradation of column RMC-CW-1 fitted in between the other two.

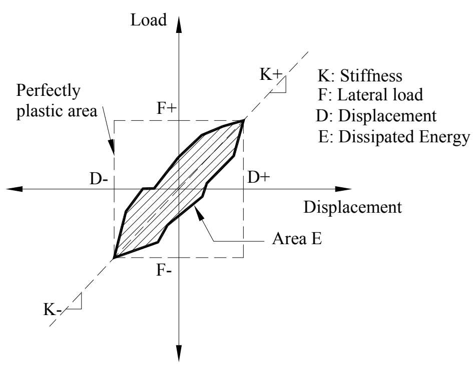

Figure 11: Determination of stiffness for each cycle

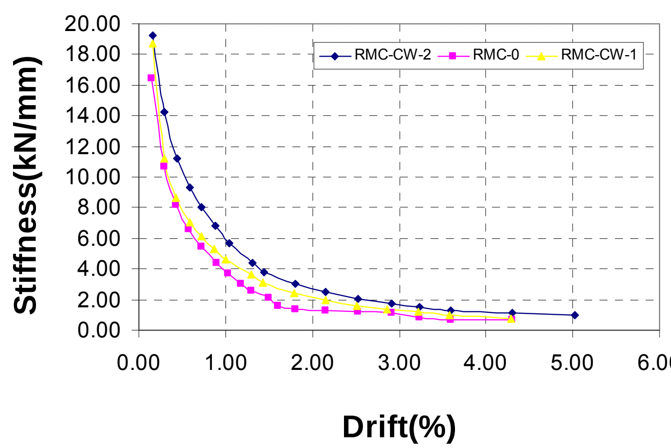

Figure 12: Stiffness degradation of columns

Ductility: The displacement ductility factor (μ_{Δ}) can be written as Δ_u/Δ_y where Δ_u is the maximum displacement and Δ_y is the yield displacement. Yield displacement, Δ_y, determined from obtained curves for lateral force and displacement. The elastic part of the force-displacement curve was defined as secant to the real curve at 75% of the maximum lateral load and reached the maximum lateral load to find the yield displacement. The failure of the column was defined at the post-peak displacement, Δ_u, where the remaining capacity has dropped to 80% of the peak load. Table 3 shows the ductility factors for each column in both directions [21].

Energy dissipation: The energy dissipation in each cycle is defined as the integration of lateral force with its displacement. Energy in each cycle was estimated by calculating the area enclosed by the corresponding load-displacement hysteretic loop as it is shown in Figure 11. The cumulative energy dissipated was obtained by summing the energy dissipated in consecutive loops. In Figure 13, drift ratio versus cumulative dissipated energy is given, and it can be seen that the retrofitted columns provided higher energy dissipation in compare to column RMC-0

Table 3: Ductilty factors for each specimen

	Push			Pull			
Specimen	Δ_{yield} (mm)	Δ_{ult} (mm)	μ_Δ	Δ_{yield} (mm)	Δ_{ult} (mm)	μ_Δ	$\mu_{\Delta(average)}$
RMC-0	13	22	1.7	10	21	2.1	1.9
RMC-CW-1	14	44	3.1	15	62	4.1	3.6
RMC-CW-2	12	80	6.7	10	72	7.2	6.9

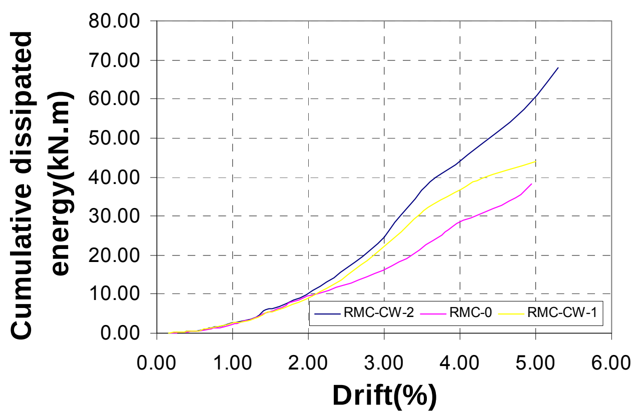

Figure 13: Drift versus cumulative energy dissipation

CONCLUSIONS

This experimental research led to the following findings:

1- Wrapping the reinforced masonry control column with full-height 1 or 2 CFRP sheets, increased the lateral load capacity of the column by about 14% and 24%, respectively.

2- Wrapping the reinforced masonry control column with full-height 1 or 2 CFRP sheets, increased the displacement ductility of the column by about 90% and 260%, respectively.

3- Wrapping the reinforced masonry control column with full-height 1 or 2 CFRP sheets, increased the cumulative energy dissipation capacity of the column by about 15% and 78%, respectively.

ACKNOWLEDGMENT

The authors wish to acknowledge the financial supports L'Association des entrepreneurs en maçonnerie du Québec (AEMQ), Canada masonry design centre (CMDC), and Tomassini et frères Ltée who assisted us through the team research project.

REFERENCES

1. Youd TL, Bardet J, Bray JD. 1999 Kocaeli, Turkey, Earthquake Reconnaissance Report, Earthquake Spectra; 2000, Supplement A to Volume 16. p. 152-170
2. Seible F, Priestley MJN, Hegemier GA, Innamorato D. Seismic retrofit of RC columns with continuous carbon fiber jackets. J Compos Constr 1997; 1(2):52–62.
3. Saadatmanesh H, Ehsani MR, Li MW. Strength and ductility of concrete columns externally reinforced with fiber composite straps. ACI Struct J 1994; 91(4):434–44.
4. Xiao Y, Ma R. Seismic Retrofit of RC circular columns using prefabricated composite jacketing. J Struct Eng 1997; 123(10):1357–64.
5. Priestley MJN, Seible F, Fyfe E. Column seismic retrofit using fiberglass/epoxy jackets. In: Neale KW, Labossiere P, editors. Proceedings of the First International Conference on Advanced Composite Materials in Bridges and Structures, Sherbrooke, Montreal, Canadian Society for Civil Engineering; 1992. p. 287–98.
6. Pessiki S, Harries K, Kestner J, Sause R, Ricles J. Axial behaviour of reinforced concrete columns confined with FRP jackets. ASCE J Compos Construct 2001; 5(4):237–45.
7. Rochette P, Labossiere P. Axial testing of rectangular column models confined with composites. ASCE J Compos Construct 2000; 4(3): 129–36.
8. Saadatmanesh H, Ehsani MR, Jin L. Seismic strengthening of circular bridge pier models with fibre composites, ACI Struct J 1996; 93(6): 639–47.
9. Parvin A, Wang W. Behaviour of FRP jacketed concrete columns under eccentric loading. ASCE J Compos Construct 2001; 5(3): 146–52.
10. K. Galal, A.Arafa, A. Ghobarah, Retrofit of RC square short columns, Journal of Engineering Structures 27 (2005) 801–813
11. Shrive PL, Azarnejad A, Tadros G, McWhinnie C, Shrive NG. Strengthening of concrete columns with carbon fibre reinforced polymer wrap. Can J Civil Eng 2003; 30:543–54.
12. Task Group 9.3. Externally Bonded FRP Reinforcement for RC Structures, fib, CEB-FIP Technical Report, fib Bulletin 14, 2001.
13. Masia MJ, Shrive NG. Carbon fibre reinforced polymer wrapping for the rehabilitation of masonry columns. Can J Civil Eng 2003; 30: 734–44.
14. Micelli F, Galati N, De Lorenzis L, La Tegola A. Confinement of natural block masonry columns using fibre reinforced polymer rebars and laminates. Proceedings of the Ninth Canadian Masonry Symposium, Fredericton, N.B., 4–6 June 2001, Department of Civil Engineering, University of New Brunswick, Fredericton, N.B. CD-ROM., 2001.
15. Theriault M, Neale KW. Design equations for axially loaded reinforced concrete columns strengthened with fibre reinforced polymer wraps. Can J Civil Eng 2000; 27:1011–20.
16. American Society of Testing and Materials (ASTM), "C270-02: Standard Specification for Mortar for Unit Masonry," 2002, West Conshohocken, Pa.
17. Canadian Standards Association, "CSA A179-04: Mortar and Grout for Unit Masonry," Mississauga, Ontario, 2004.
18. American Society of Testing and Materials (ASTM), "C476-02: Standard Specification for Grout for Masonry," 2002, West Conshohocken, Pa.
19. American Society of Testing and Materials (ASTM), "C1314-02: Standard Test Method for Compressive Strength of Masonry Prisms," 2002, West Conshohocken, Pa.
20. American Society of Testing and Materials (ASTM), "C518-02: Standard Test Method for Flexural Bond Strength of Masonry," 2002, West Conshohocken, Pa.

21. Park R. Evaluation of ductility of structures and structural assemblages from laboratory testing. Bull New Zeal Nat Soc Earthquake Eng 1989; 22(3).